ANNALS OF
BOTANY
Founded 1887

PART OF THE FOCUS ISSUE ON PLANT DEFENCE AND STRESS REPSONSE

# Identification of salicylic acid-independent responses in an Arabidopsis phosphatidylinositol 4-kinase beta double mutant

**Tetiana Kalachova**[1,5†], **Martin Janda**[1,2†], **Vladimír Šašek**[1], **Jitka Ortmannová**[1‡], **Pavla Nováková**[1,2],
**I. Petre Dobrev**[1], **Volodymyr Kravets**[3], **Anne Guivarc'h**[4], **Deborah Moura**[5], **Lenka Burketová**[1], **Olga Valentová**[2]
**and Eric Ruelland**[4,5*]

[1]*Institute of Experimental Botany, The Czech Academy of Sciences, Prague 160 000, Czech Republic,* [2]*University of Chemistry and Technology, Department of Biochemistry and Microbiology, Prague 166 28, Czech Republic,* [3]*Institute of Bioorganic Chemistry and Petrochemistry, National Academy of Sciences of Ukraine, 02094 Kiev, Ukraine,* [4]*CNRS, Institut d'Ecologie et des Sciences de l'Environnement de Paris, UMR 7618, Créteil, France and* [5]*Université Paris-Est, UPEC, Institut d'Ecologie et des Sciences de l'Environnement de Paris, Créteil, France*
[†] *Equal first authors.*
[‡] *Present address: Department of Plant Biology, Swedish University of Agricultural Sciences, SE-750 07 Uppsala, SWEDEN*

\* *For correspondence. E-mail* eric.ruelland@upmc.fr

• **Background and Aims** We have recently shown that an *Arabidopsis thaliana* double mutant of type III phosphatidylinositol-4-kinases (PI4Ks), *pi4kβ1β2*, constitutively accumulated a high level of salicylic acid (SA). By crossing this *pi4kβ1β2* double mutant with mutants impaired in SA synthesis (such as *sid2* impaired in isochorismate synthase) or transduction, we demonstrated that the high SA level was responsible for the dwarfism phenotype of the double mutant. Here we aimed to distinguish between the SA-dependent and SA-independent effects triggered by the deficiency in *PI4Kβ1* and *PI4Kβ2*.
• **Methods** To achieve this we used the *sid2pi4kβ1β2* triple mutant. High-throughput analyses of phytohormones were performed on this mutant together with *pi4kβ1β2* and *sid2* mutants and wild-type plants. Responses to pathogens, namely *Hyaloperonospora arabidopsidis*, *Pseudomonas syringae* and *Botrytis cinerea*, and also to the non-host fungus *Blumeria graminis*, were also determined. Callose accumulation was monitored in response to flagellin.
• **Key Results** We show here the prominent role of high SA levels in influencing the concentration of many other tested phytohormones, including abscisic acid and its derivatives, the aspartate-conjugated form of indole-3-acetic acid and some cytokinins such as *cis*-zeatin. We show that the increased resistance of *pi4kβ1β2* plants to the host pathogens *H. arabidopsidis*, *P. syringae* pv. *tomato* DC3000 and *Bothrytis cinerea* is dependent on accumulation of high SA levels. In contrast, accumulation of callose in *pi4kβ1β2* after flagellin treatment was independent of SA. Concerning the response to *Blumeria graminis*, both callose accumulation and fungal penetration were enhanced in the *pi4kβ1β2* double mutant compared to wild-type plants. Both of these processes occurred in an SA-independent manner.
• **Conclusions** Our data extensively illustrate the influence of SA on other phytohormone levels. The *sid2pi4kβ1β2* triple mutant revealed the role of PI4Kβ1/β2 *per se*, thus showing the importance of these enzymes in plant defence responses.

**Keywords:** pi4kβ1β2/PI4Ks, callose, salicylic acid, phytohormones, isochorismate synthase 1, biotic stress, pathogens, *Arabidopsis thaliana*.

## INTRODUCTION

Salicylic acid (SA) is a phytohormone that has a role in many plant physiological processes, although this has mainly been documented in plant responses to biotic stress when SA accumulates within tissues, both at the site of attack and in a systemic manner (Vlot *et al.*, 2009; Janda and Ruelland, 2015). In plants, SA is biosynthesized via two pathways. One is dependent on phenylalanine ammonia-lyase (PAL; EC 4.3.1.24), which catalyses the conversion of phenylalanine to *trans*-cinnamic acid. In the other pathway, the key enzyme is isochorismate

synthase (ICS; EC 5.4.4.2), which catalyses the isomerization of chorismate to isochorismate (Dempsey *et al.*, 2011). The ICS-dependent pathway was shown to be responsible for most SA accumulation upon pathogen attack. In *Arabidopsis thaliana*, two ICS isoforms exist, but the major role in SA biosynthesis is played by ICS1. The *ICS1* mutant is known as *sid2* for *salicylic acid induction deficient 2* (Wildermuth *et al.*, 2001; Wagner *et al.*, 2013; Cui *et al.*, 2017). When SA levels increase, downstream signalling events are triggered, and the best described molecular pathway is dependent on NONEXPRESSOR

OF PATHOGENESIS RELATED 1 (NPR1). Upon SA action, homo-oligomeric NPR1 protein undergoes dissociation by reduction and the resulting monomers move into the nucleus where they interact with TGA-transcription factors to induce the expression of SA responsive genes. An NPR1-independent pathway also exists in response to SA (Janda and Ruelland, 2015). The activation of SA signalling pathways leads to robust changes in the plant transcriptome, including defence-related genes (Seyfferth and Tsuda, 2014). Among the immune responses affected by changes in SA levels or by SA treatments is the accumulation of callose (Kohler *et al.*, 2002; Dong *et al.*, 2008; Antignani *et al.*, 2015), a (1,3)-*β*-glucan occurring in plant cell walls.

The signalling pathways triggered by SA remain the subject of current research. We have shown that phosphoinositides, the phosphorylated derivatives of phosphatidylinositol (PI), are involved in SA transduction. Indeed, PI can be phosphorylated at the D4 position of the inositol ring by phosphatidylinositol-4-kinases (PI4Ks) thus leading to phosphatidylinositol 4-phosphate (PI4P), which can be phosphorylated further to phosphatidylinositol-4,5-bisphosphate (PI-4,5-$P_2$). There are two types of PI4Ks according to their primary sequences and pharmacological sensitivities. Type II PI4Ks are inhibited by adenosine while type III PI4Ks are inhibited by micromolar concentrations of wortmannin, a steroid metabolite produced by the fungus *Penicillium funiculosum* (Nakanishi *et al.*, 1995; Balla, 2007; Krinke *et al.*, 2007). From the *A. thaliana* genome, 12 putative PI4K isoforms have been identified. Eight belong to type II (AtPI4Kγ1–8) and four belong to type III (AtPI4Kα1 and α2, AtPI4Kβ1 and β2) (Delage *et al.*, 2012; Janda *et al.*, 2014). We have shown that type III PI4Ks are activated when *A. thaliana* suspension cells respond to SA, thus leading to an increase in PI4P and PI-4,5-$P_2$ (Krinke *et al.*, 2007). PI-4,5-$P_2$ can act as a cofactor to some phospholipase Ds (Pappan *et al.*, 1998). Interestingly, there is overlap between SA-responsive genes controlled by PI4Ks and those controlled by phospholipase Ds, leading to the working model that in response to SA, PI4P and PI-4,5-$P_2$ are produced with PI-4,5-$P_2$ acting as a cofactor for a phospholipase D, whose product, PA, will trigger a signalling cascade (Krinke *et al.*, 2009; Kalachova *et al.*, 2016).

To better characterize the role of PI4Ks in the response to SA, we have used *A. thaliana* mutants altered in type III PI4Ks. We previously worked on a double mutant defective in the two PI4Kβ genes. Surprisingly, *pi4kβ1β2* exhibited a constitutively high SA level that resulted in constitutive high transcription of SA-responsive genes such as *PR-1* (PATHOGENESIS RELATED 1). Therefore, PI4Ks are not only involved in SA transduction but they can also impact SA concentration. Furthermore, this double mutant exhibited dwarfism and was more resistant to the bacterial pathogen *Pseudomonas syringae* pv. *maculicola* ES4326 (Sasek *et al.*, 2014). The *pi4kβ1β2* plant was crossed with mutants impaired in components of SA synthesis (*sid2*, impaired in *ICS1* expression; *eds1*), SA transduction (*npr1*) or a mutant expressing bacterial SA-hydroxylase (NahG) that degrades SA to catechol. The resulting triple mutants allowed us to conclude that the dwarf phenotype of *pi4kβ1β2* plants was dependent on SA accumulation and its transduction via the NPR1 pathway (Janda *et al.*, 2014; Sasek *et al.*, 2014).

In the present study, our aim was to identify amongst the cellular and physiological processes affected by the deficiency of PI4Kβ1β2 those that were either SA-dependent or SA-independent. To achieve this, we used the *sid2pi4kβ1β2* triple mutant that does not accumulate SA and exhibits wild-type-sized rosettes (Sasek *et al.*, 2014). In this mutant, the effects of PI4K*β1* and PI4K*β2* mutations would not be masked by high SA levels. We showed that hormonal levels and pathogen resistance were mainly dependent on SA. However, we could show that *sid2pi4kβ1β2* plants accumulated higher amounts of callose in response to *flg22* and wounding. Interestingly, this SA-independent callose accumulation was also observed during early stages of interactions with *Blumeria graminis* when penetration was observed. Our data suggest that PI4Ks are involved in plant immune responses not only through SA accumulation but also via SA-independent processes.

## MATERIALS AND METHODS

### Plant material, growth conditions

In this study, we used the following genotypes of *A. thaliana*: Columbia-0 (WT), *sid2-3* (Gross *et al.*, 2006), *npr1-1* (Cao *et al.*, 1997), *NahG* (Delaney *et al.*, 1994), *pi4kβ1β2* (SALK_040479/SALK_09069; Preuss *et al.*, 2006), *sid2pi4kβ1β2*, *NahGpi4kβ1β2* and *npr1pi4kβ1β2* mutants previously described (Sasek *et al.*, 2014).

All plants were cultivated in Jiffy 7 peat pellets at 22 °C with 70 % relative humidity. All plants were watered without additional fertilizers. Plants were routinely cultivated in daily cycles of 10 h light (100–130 μE m$^{-2}$ s$^{-1}$) and 14 h dark. Plants that would be used for hormonal analysis or transcription analysis were cultivated under 16 h light (130–150 μE m$^{-2}$ s$^{-1}$) and 8 h dark.

### Pathogen inoculation

Two-week-old plants grown at high density in one pot were sprayed with *Hyaloperonospora arabidopsidis NoCo2* spores (~100 spores μL$^{-1}$). The infected plants were cultivated in closed transparent plastic boxes at high humidity for 6 d under 16 h light/8 h dark (100–130 μE m$^{-2}$ s$^{-1}$) at 19 °C. For analysis, leaves collected from one pot were considered as one sample (for each genotype, 11 samples were analysed). Spores were counted under a microscope using a Bürker chamber and expressed as relative spore number (%), where relative spore number for a given control genotype (WT or *sid2*) was set to 100 %. The spores were counted as spores per milligram of tissue fresh weight. The experiments (WT vs. *pi4kβ1β2* and *sid2* vs. *sid2pi4kβ1β2*) were conducted independently.

Inoculation with *P. syringae* was performed according to Katagiri *et al.* (2002) with modifications. Bacteria were cultivated overnight on King's B medium plates containing rifampicin (50 μg μL$^{-1}$). *P. syringae* pv. *tomato* DC3000 (*Pst* DC3000) and *P. syringae* pv. *tomato* DC3000 AvrRpt2 (*Pst* DC3000 AvrRpt2) were taken from the respective plate and resuspended in 10 mM MgCl$_2$ to give an OD$_{600}$ of 0.001. Four-week-old plants were infiltrated with this suspension.

One disc (6 mm) from one leaf, three leaves at a similar developmental stage from one plant and three plants were collected as one sample of one genotype at 0 days post-inoculation (dpi) and 3 dpi (3 dpi only for *Pst* DC3000; 2 dpi for *Pst* DC3000 AvrRpt2). Leaf discs were ground in 10 mM $MgCl_2$ and decimal dilutions were made. Colony forming units were counted.

Four-week-old *A. thaliana* plants were treated with 6 μL drops containing *Botrytis cinerea* BMM spores ($5 \times 10^4$ spores $mL^{-1}$) by applying a single drop to each leaf, with three leaves at a similar developmental stage inoculated for each plant. Treated plants were placed into closed plastic boxes and kept in low light (16 h light/8 h dark, 21 °C; 10–μE $m^{-2}$ $s^{-1}$) for 56 h post-inoculation (hpi).

*Blumeria graminis* f. sp. *hordei* (*Bgh*) was cultivated continuously on fresh barley ('Golden promise') grown under short day conditions (19 °C, 10/14 h, 50 % humidity, at a light intensity of 70 μmol $m^{-2}$ $s^{-1}$). Plants, ~4 weeks old, were inoculated by spreading spores from infected barley onto the adaxial side of their leaves (from leaf to leaf). The 5th–6th leaves were cut off at selected times hours post-inoculation (hpi) and cleared with 96 % ethanol or chloral hydrate. For penetration rate, fungal structures were stained with 250 mg $mL^{-1}$ trypan blue in a lactophenol/ethanol solution (Vogel and Somerville, 2000). Stained leaves were observed by classical epifluorescence microscopy or bright-field microscopy using a Zeiss AxioImager ApoTome2 (objective 100×).

### Callose deposition

Four-week-old *A. thaliana* plants were treated for 24 h with 100 nM flg22 or infiltrated with *Pst* DC3000. Distilled water infiltration was used as a control (mock) treatment. Infiltrated leaves were decoloured in ethanol/glacial acetic acid (3:1, v/v). The leaves were then rehydrated in successive baths of 70 % ethanol (at least 1 h), 50 % ethanol (at least 1 h), 30 % ethanol (at least 1 h) and water (at least 2 h). Leaves were stained for 4 h with 0.01 % aniline blue in 150 mM $K_2HPO_4$, pH 9.5. Callose deposition was observed by fluorescence microscopy using a Zeiss AxioImager ApoTome2 (objective 10×). In *Bgh* infection analysis, we calculated only callose spots using the high circularity function of the measurement settings at an interval of 0.5–1 which allowed us to distinguish only the cells with the size exclusion limit for spots corresponding to either encased haustoria or enormous papilla. Images were processed with ImageJ software. At least four leaves from three independent plants were analysed for each variant.

### RNA extraction and qPCR analysis

Plant tissues were homogenized in 2-mL screw-cap tubes containing 1 g of 1.3-mm-diameter silica beads using a FastPrep-24 instrument (MP Biomedicals, USA). Total RNA was isolated using a Spectrum Plant Total RNA kit (Sigma-Aldrich, USA) and treated with a DNA-free kit (Ambion, USA). Subsequently, 1 μg of RNA was converted to cDNA with M-MLV RNase H– Point Mutant reverse transcriptase (Promega Corp., USA) and an anchored oligo dT21 primer (Metabion, Germany). Gene transcription was quantified by qPCR using a LightCycler 480 SYBR Green I Master kit and a LightCycler 480 (Roche, Switzerland). The PCR conditions employed were 95 °C for 10 min followed by 45 cycles of 95 °C for 10 s, 55 °C for 20 s and 72 °C for 20 s. Melting curve analyses were then carried out. Relative transcription was normalized to the housekeeping genes *SAND* or *TIP41* (Czechowski *et al.*, 2005). Primers were designed using PerlPrimer v1.1.21 (Marshall, 2004). The primers used were CalS1_FP, AAGAGCGGAGGGTCACTTTG; CalS1_RP, GGCGACACGAATAGACGGAT; CalS12_ FP, TTCACTCCGTTTTCCCGAGG; and CalS12_RP, GGAGAGAGACGCATCTGAGC.

### Analysis of plant hormones

Plant hormones were extracted from 100 mg of frozen tissues and their concentrations were determined as previously described (Dobrev and Vankova, 2012; Dobrev and Kaminek, 2002) after the addition of appropriate internal standards. Hormone analysis was carried out on four samples, each taken from three plants. Briefly, samples were homogenized in tubes with 1.3-mm silica beads using a FastPrep-24 instrument (MP Biomedicals). Samples were then extracted with a methanol/ $H_2O$/formic acid (15:4:1, by vol.) mixture, which was supplemented with stable isotope-labelled phytohormone internal standards (10 pmol per sample) in order to check recovery during purification and to validate the quantification. The clarified supernatants were subjected to solid phase extraction using Oasis MCX cartridges (Waters Co., USA). The eluates were evaporated to dryness and the generated solids were dissolved in 30 μL of 15 % (v/v) acetonitrile in water. Hormones were separated and quantified by Ultimate 3000 high-performance liquid chromatography (Dionex, USA) coupled to a 3200 Q TRAP hybrid triple quadrupole/linear ion trap mass spectrometer (Applied Biosystems, USA) as described by Dobrev *et al.* (2017). Metabolite levels were expressed in pmol/g fresh weight (f. wt).

### Statistical analysis

At least three independent biological replicates were performed for all experiments. Statistical analysis was conducted by paired *t*-test or ANOVA with Tukey honestly significant difference (HSD) multiple mean comparison *post hoc* test. The number of analysed samples was specified for each condition. The correlation matrix for hormonal levels was prepared using R-software *Hmisc* and *corrplot* packages based on the Pearson correlation (R Core Team, 2014).

## RESULTS

### The pi4kβ1β2 *double mutant has altered phytohormonal levels*

Our goal was to identify SA-dependent and SA-independent processes triggered by the double *pi4kβ1β2* mutation. To do so, we used a *sid2pi4kβ1β2* triple mutant. If a process triggered by the double *pi4kβ1β2* mutation is SA-dependent, then it should disappear in the *sid2pi4kβ1β2* triple mutant. On the

other hand, if a process triggered by the double *pi4kβ1β2* mutation is SA-independent, then it should still be observed in the *sid2pi4kβ1β2* triple mutant.

Because the main effect of the double *pi4kβ1β2* mutation was on the level of SA, we decided to quantify a broad spectrum of phytohormones in the *sid2pi4kβ1β2* triple mutant. The hormone levels obtained were compared to those of *pi4k β1β2*, *sid2* and WT plants. A first look allowed us to establish that the *pi4k β1β2* double mutation does not impact only SA levels. Many hormone-related metabolites showed significantly different levels in *pi4k β1β2* plants when compared to WT plants while most of them remained at WT levels in *sid2pi4kβ1β2*

(Supplementary Data Table S1). In our previous study, we created an additional triple mutant by crossing *pi4kβ1β2* with an *NahG* mutant impaired in SA accumulation: *NahGpi4kβ1β2* (Sasek *et al.*, 2014). To confirm and to strengthen the results obtained with *sid2pi4kβ1β2*, we also quantified phytohormones in *NahGpi4kβ1β2*, together with their corresponding single mutants (Table S1). From these data, we built a correlation matrix (Fig. 1). Many hormone levels were correlated to higher SA levels (Pearson correlation >0.7) as seen for the abscisic acid (ABA) derivatives such as 9-hydroxy-ABA (9OH-ABA), phaseic acid (PA) and dihydrophaseic acid (DPA). However, the high levels of DPA, PA and 9OH-ABA observed in *pi4kβ1β2*
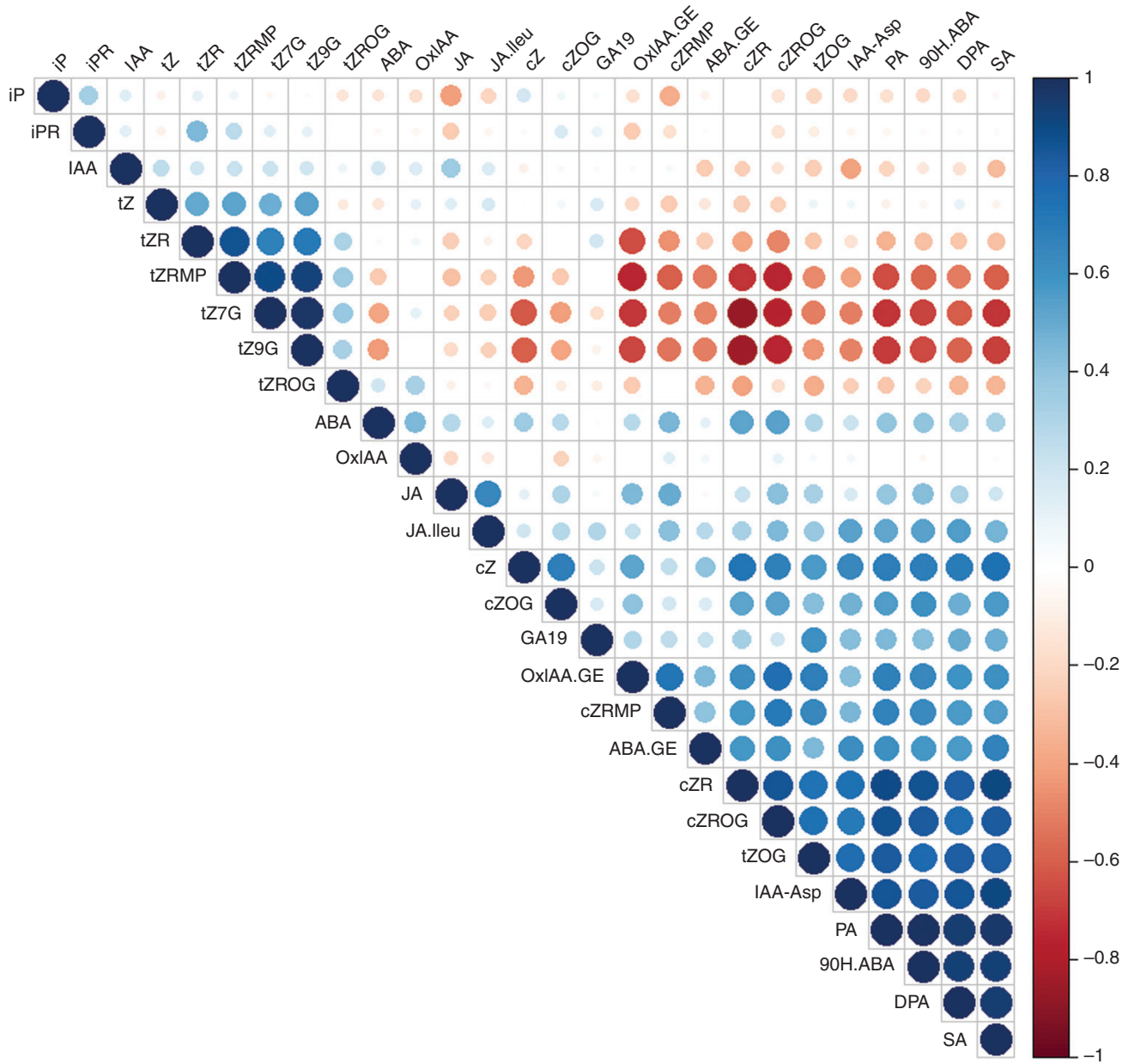


FIG. 1. Correlation matrix between phytohormone levels. The matrix was built using the Pearson correlation of 27 hormone-related metabolites from 24 independent samples corresponding to six genotypes (WT, *sid2*, *NahG*, *pi4kβ1β2*, *sid2pi4kβ1β2* and *NahGpi4kβ1β2*; four plants per genotype). Positive correlations are displayed in blue and negative correlations in red. Colour intensity and the size of the circles are proportional to the correlation coefficients. Red rectangles highlight the correlation between SA and other hormones.

vs. WT were no longer seen in the triple mutants with low SA; therefore, these metabolite levels were controlled by SA in the *pi4kβ1β2* double mutant (Fig. S1A).

Because the main genetic pathway of the SA response is controlled by NPR1, we investigated whether the hormonal control of SA was NPR1-dependent. This was achieved using a previously generated *npr1pi4kβ1β2* triple mutant where the SA level was 30-fold that of the WT and 4-fold that of *pi4kβ1β2*. Interestingly, levels of DPA, PA and 9OH-ABA were still high in *npr1pi4kβ1β2*, showing that the effect of SA on these metabolites was only partially NPR1-dependent. Note that ABA levels did not correlate with SA (Pearson correlation 0.3), indicating that the action of SA on ABA derivatives is probably not directly connected to the biosynthesis of ABA, but with its metabolism.

Other hormones with high Pearson correlations to SA were the Asp conjugated form of indole-3-acetic acid (Asp-IAA) and some cytokinins. The increased level of Asp-IAA observed in *pi4kβ1β2* was no longer observed in the triple mutants with low SA. However, it was still visible in the *npr1pi4kβ1β2* triple mutant, suggesting that this metabolite is controlled by SA but it is only partially NPR1-independent (Supplementary Data Fig. S1B). The pattern of IAA was different from that of Asp-IAA, suggesting that SA control of Asp-IAA is on aspartate conjugation. As for cytokinins, the increase in *cis*-zeatin (cZ), *cis*-zeatin-riboside (cZR), *cis*-zeatin-7-N-glucoside (cZ7G), *cis*-zeatin-riboside-*O*-glucoside (cZROG) and *trans*-zeatin-*O*-glucoside (tZOG) and the decrease in *trans*-zeatin-7-N-glucoside (tZ7G) and *trans*-zeatin-9-N-glucoside (tZ9G) in the *pi4kβ1β2* double mutant were SA-driven. In contrast to the other hormones tested, SA's action on tZROG appeared to be partially independent of NPR1 (Fig. S1C).

We identified one hormone for which its level was altered in *pi4kβ1β2* plants independently of SA: the increase in oxIAA-GE observed in *pi4kβ1β2* was still visible in the triple mutants with low SA. Note that oxIAA did not follow the same pattern (Supplementary Data Fig. S2).

### *Pathogen resistance, of* pi4kβ1β2 *plants is SA-dependent*

At the hormonal level, our data show that the major change induced by the *pi4kβ1β2* double mutation was an increase in SA, with this change determining the levels of many other hormones. Because a major role of SA is related to biotic stress responses, we reasoned that processes related to biotic stress, dependent or not on SA, might also be altered in the double mutant.

Whether the PI4K double mutation *per se* was accompanied by an enhanced resistance to pathogens was investigated. Comparing resistance in *sid2pi4k β1β2* plants to that in *pi4k β1β2* or *sid2* would allow us to distinguish between the effectiveness of SA-dependent and SA-independent responses. Therefore, different pathogens with different life-styles (biotrophs, hemibiotrophs and necrotrophs) were tested (Glazebrook, 2005). The *pi4kβ1β2* double mutant plants were more resistant to the biotroph *H. arabidopsidis NoCo2* compared to WT. However, *sid2pi4kβ1β2* resistance was similar to that of *sid2* plants (Fig. 2A). We then studied resistance to the hemibiotroph *P. syringae* pv. *tomato* DC3000 in its wild type (*Pst* DC3000) or AvrRpt2-expressing form (*Pst* DC3000

AvrRpt2). *Pst* DC3000 AvrRpt2 leads to a strong effector-triggered immunity (ETI) response compared to *Pst* DC3000. With both forms, pathogen development was reduced in *pi4k β1β2* plants compared to the WT while *sid2pi4kβ1β2* resistance was comparable to that of *sid2* and lower than WT plants (Fig. 2B, Supplementary Data Fig. S3). Unexpectedly, the double mutant also showed an increased resistance to the necrotroph *Botrytis cinerea* which was also SA-dependent as *sid2pi4kβ1β2* resistance was similar to that of *sid2* and WT plants (Fig. 2C). For each pathogenic assay, triple mutant resistance was similar to *sid2*, indicating that SA-dependent pathways were dominant in the immune response. Putative mechanisms regulated by PI4K activity alone were not sufficient to establish pathogen resistance.
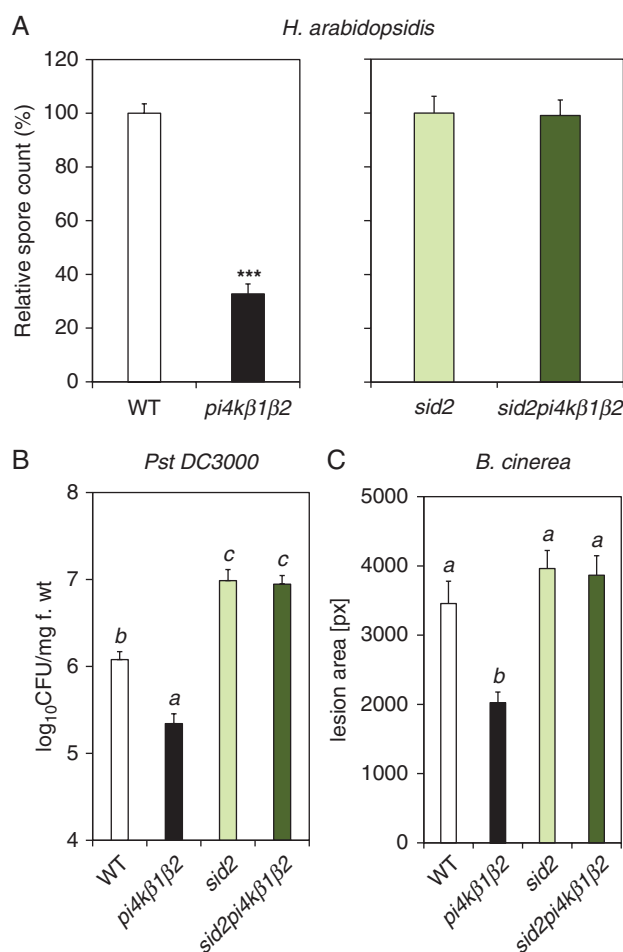


FIG. 2. Resistance to biotic stresses of *pi4kβ1β2* and s*id2pi4kβ1β2* mutants. (A) Resistance to the biotroph *Hyaloperonospora arabidopsidis*. (B) Resistance to the hemibiotroph *Pseudomonas syringae* pv. *syringae* DC3000. Infiltration treatment of 4-week-old-plants, with six independent samples. (C) Resistance to the necrotroph *Botrytis cinerea*. Four- to 5-week-old *A. thaliana* were inoculated with a 6-μL drop containing spores of *Botrytis cinerea* (50 000 spores $mL^{-1}$), placed into a plastic box and kept in the dark for 56 h. Statistical differences between the genotypes for B and C were assessed using ANOVA, with a Tukey honestly significant difference (HSD) multiple mean comparison *post hoc* test. Different letters indicate a significant difference, Tukey HSD, *P* < 0.05, *n* = 10 for A, *n* = 7 for B and *n* = 27 for C. ***Indicate difference from WT, *t*-test, *P* < 0.001.

*The enhanced level of basal callose deposition in* pi4kβ1β2 *is mainly SA-dependent, while stress-induced callose accumulation is not*

SA levels modulate numerous processes associated with immune responses, including the strengthening of leaf tissues and particularly cell walls around the infection site by lignification and callose accumulation (Voigt, 2014). Interestingly, SA pretreatment also has a positive effect on flagellin-induced callose accumulation (Yi *et al.*, 2014). We therefore studied callose levels, accumulated in leaf tissues in response to treatment with the flagellin epitope (flg22). We first studied callose accumulation in the absence of flg22 treatment (control; Fig. 3A). The *pi4kβ1β2* double mutant exhibited a constitutively high level of callose deposition, as previously shown (Antignani *et al.*, 2015). We were able to show that a spatial pattern in callose accumulation existed, as the examination of different regions of interest (ROI) indicated a higher accumulation in the upper part of the leaf edges (Fig. 3B).

Callose accumulation was then assessed in either mock-infiltrated or flg22-treated plants (Fig. 4). In this case, callose accumulation was much higher in *pi4kβ1β2* when compared to WT plants (Fig. 4). The *sid2pi4kβ1β2* triple mutant was used to investigate whether high callose deposition in the double mutant depended on its high SA level. For mock treatments, callose deposition was much lower in *sid2pi4kβ1β2* compared to *pi4kβ1β2* plants. This provides arguments for an SA-dependent higher basal callose deposition. This was confirmed by the response to flg22. In WT plants, flg22 induced 20 times more callose compared to control mock infiltrations. Again, the callose level in *pi4kβ1β2* was higher (two-fold) compared to WT plants. This increase was reduced when the *sid2* mutation was introduced into the *pi4kβ1β2* double mutant as the level in the triple mutant was about two-fold lower than in the double mutant and in the same range as the WT level. This indicated that SA was a major inducer of callose accumulation in the *pi4kβ1β2* genotype context. Yet, the *sid2pi4kβ1β2* triple mutant exhibited a higher callose deposition than *sid2* plants. Therefore, the *pi4kβ1β2* double mutation *per se* had a role in the high callose accumulation observed in the *pi4kβ1β2* double mutant.

We also studied callose accumulation in leaf tissues in response to mechanical wounding (Supplementary Data Fig. S4). Again, in response to wounding, the PI4K double mutation enhanced callose accumulation via an SA-dependent pathway.
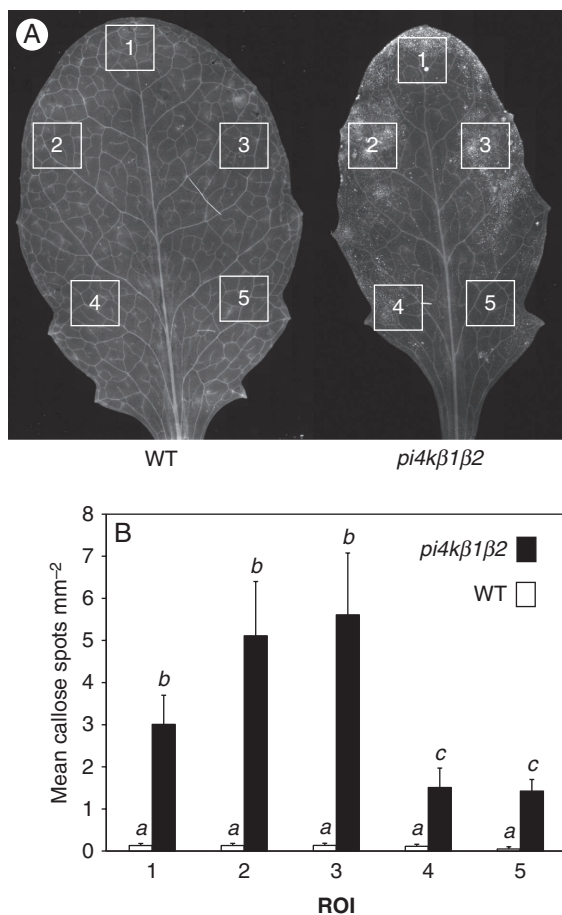


FIG. 3. Pattern of callose accumulation in *pi4kβ1β2* leaves. (A) Aniline blue staining, and fluorescence microscopy. Scale bar = 500 μm. (B) Callose particles accumulated in different ROI. The squares represent the ROI. Data are presented as means ±s.e.m. Statistical differences were assessed using a two-way ANOVA, with a Tukey honestly significant difference (HSD) multiple mean comparison *post hoc* test. Different letters indicate a significant difference, Tukey HSD, $P < 0.05$. $n = 11$.
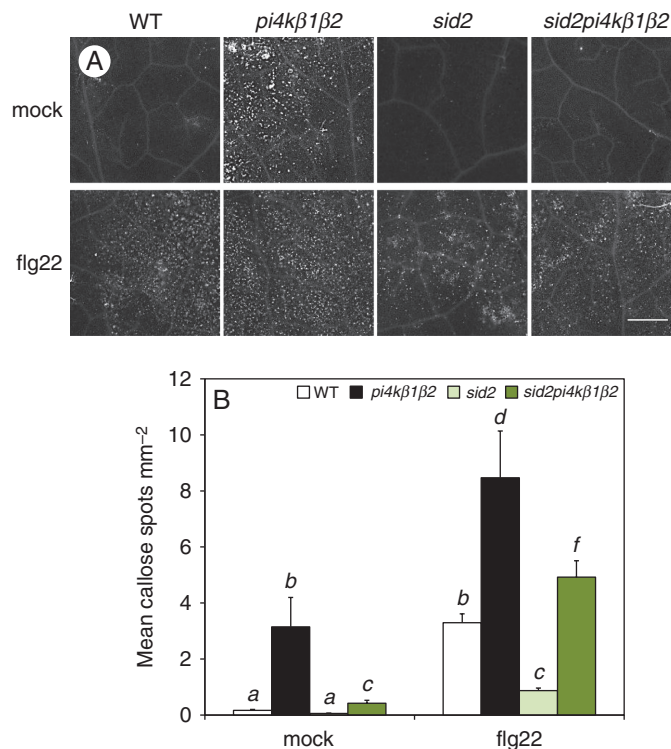


FIG. 4. Callose deposition in response to flagellin. (A) Representative images of callose accumulated in leaves of 4-week-old *A. thaliana* plants by aniline blue staining, 24 h after infiltration with 0.1 μM flg22 or mock infiltration. Scale bar = 1cm. (B) Quantification of callose particles. Values represent an average of five ROI. Data are presented as means +s.d. For each treatment, statistical differences between the genotypes were assessed using a one-way ANOVA, with a Tukey honestly significant difference (HSD) multiple mean comparison *post hoc* test. Different letters indicate a significant difference, Tukey HSD, $P < 0.01$, $n = 4$.

Whether callose overaccumulation correlated with the transcription of callose synthases (*CalSs*) was then investigated. Among 12 callose synthases, *CalS1* and *CalS12* have been shown to be related to SA and/or biotic stresses (Dong *et al.*, 2008). The transcript levels of *CalS1* and *CalS12* were tested by qPCR in WT, *pi4kβ1β2*, *sid2* and *sid2pi4kβ1β2* plants treated or not with flg22. No correlation was observed between *CalS1* and *CalS12* transcript levels and callose accumulation (Supplementary Data Fig. S5).

### pi4kβ1β2 *has altered non-host resistance that is SA-independent*

The establishment of non-host resistance is based on different mechanisms, involving vesicular secretion as well as callose accumulation (Collins *et al.*, 2003; Assaad *et al.*, 2004; Takemoto *et al.*, 2006; Böhlenius *et al.*, 2010; Lee *et al.*, 2017). To study the role of PI4K in such responses, we tested penetration success and callose production in response to the non-host pathogen *Blumeria graminis* f. sp. *hordei* (*Bgh*). In *Bgh/A. thaliana* interactions, callose accumulates in defensive papillae and haustorial encasements or around dead cells (Jacobs *et al.*, 2003; Assaad *et al.*, 2004; Ellinger *et al.*, 2014). The enhanced number of plant cells with developed haustoria

or dead cells reflects the penetration success of fungal hyphae (Fig. 5A). In our experiments a higher penetration correlated with greater callose accumulation in the plant tissue. In particular, the *pi4kβ1β2* double mutant showed an enhanced successful penetration of *Bgh* 24 hpi, as seen by the enhanced number of haustoria and dead cells. A similar defect in penetration resistance was seen in *sid2/pi4kβ1β2*, indicating the SA-independent character of this phenomenon (Fig. 5B). Both *pi4kβ1β2* and *sid2/pi4kβ1β2* accumulated more callose (Fig. 5C) and over larger areas compared to WT plants (Fig. 5C, D). Thus, the lower penetration resistance accompanied by callose accumulation in *pi4kβ1β2* was independent of the SA pathway.

## DISCUSSION

The aim of this study was to investigate SA-dependent and SA-independent processes caused by the *pi4k β1β2* double mutation. As previously shown (Sasek *et al.*, 2014), this mutant accumulates a constitutively high level of SA. In *pi4k β1β2*, SA biosynthesis is dependent on ICS1, as demonstrated by an absence of SA accumulation in the *sid2pi4kβ1β2* triple mutant with impaired *ICS1* transcription (Sasek *et al.*, 2014). This was confirmed with the hormone analysis described in
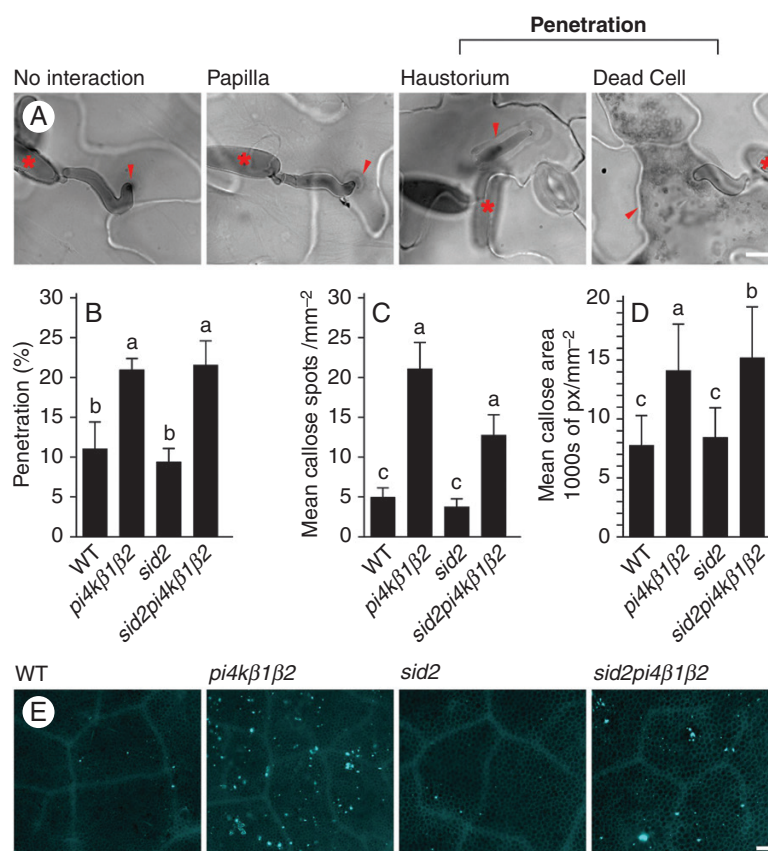


Fɪɢ. 5. Resistance of *pi4kβ1β2* to penetration by the non-host pathogen *Blumeria graminis* f. sp. *hordei* (*Bgh*). (A) Four types of interactions counted in the penetration success analysis after trypan blue staining. Scale bar = 5 µm. (B) Data showing penetration success of *Bgh* 24 hpi in each genotype: the mean number of cells with either haustoria or dead cells, respectively. (C) Data showing mean area of a callose spot per mm$^2$ at 24 hpi after interaction with *Bgh* spores. (D) Data showing mean area of a callose spot per mm$^2$ at 24 hpi after interaction with *Bgh* spores. Data for B, C and D were processed by ANOVA, with a Tukey honestly significant difference (HSD) multiple mean comparison *post hoc* test, the data represent one independent experiment, and the experiment was repeated four times. Letters indicate a significant difference, Tukey HSD, $P < 0.01$. (E) Pictures demonstrating callose staining with aniline blue 24 hpi with *Bgh*. Scale bar = 100 µm.

the present study. The *sid2pi4kβ1β2* triple mutant lacking high SA was used as a tool to distinguish between SA-dependent and SA-independent effects caused by the double mutation in *pi4kβ1β2.*

We first measured phytohormonal levels in fully developed leaves of 4-week-old *A. thaliana* WT, *pi4kβ1β2*, *sid2* and *sid2pi4kβ1β2* plants. To our knowledge, this is the broadest phytohormonal study carried out with an SA over-accumulating mutant (in our case *pi4kβ1β2*) and its comparison with a plant having the same background but with an impaired SA pathway (*sid2pi4kβ1β2*). The level of 15 hormone derivatives (excluding SA) was altered in *pi4k β1β2* compared to WT leaves. For 13 of these, this was SA-dependent. We identified two metabolites, *cis*-zeatin-riboside-5'-monophosphate and glucosylesters of oxindole-3-acetic acid, for which the *pi4k β1β2* double mutation effect was SA-independent. The same conclusions were also reached with another triple mutant, *NahGpi4kβ1β2*. Amongst the hormones controlled by SA were ABA derivatives such as DPA, PA and 9OH-ABA. As ABA levels did not correlate with SA, the action of SA on ABA derivatives did not appear to act on ABA biosynthesis but on its metabolism. Such an effect of SA on ABA catabolism is poorly described. A slight induction of ABA 8'-hydroxylase expression was observed after 24 h of SA treatment of rice seedlings (Mega *et al.,* 2015). In an *A. thaliana cpr22* mutant (*constitutive expressor of PR genes 22*), the increase of SA and ABA levels due to a high to low humidity shift was also followed by the SA-dependent expression of genes encoding ABA-metabolizing enzymes (Mosher *et al.,* 2010).

Other hormones displaying a high correlation to SA were Asp-IAA and some cytokinins (SA positively controlled cZROG and tZOG and negatively controlled tZ7G and tZ9G). The pattern of IAA was different from that of Asp-IAA, suggesting that SA control of Asp-IAA was on aspartate conjugation. Aspartate conjugation is catalysed by GH3.2-GH3.6 (Normanly, 2010), with our transcriptome data obtained with *in vitro* grown *pi4kβ1β2* seedlings (Sasek *et al.,* 2014) indicating that *GH3.3* (At2g23170) was overexpressed in the double mutant. It would be interesting to investigate whether it was responsible for the Asp-IAA /SA correlation in our double mutant.

Our results demonstrate the major role of hormonal crosstalk between SA and other hormones but only a minor role of impairment of PI4Kβ1/β2 *per se*. Because a major role of SA is related to responses to biotic stresses, we reasoned that other processes related to biotic stress, whether SA-dependent or not, could also be altered in the double mutant. We tested the resistance of WT, *pi4kβ1β2*, *sid2* and *sid2pi4kβ1β2* plants to representative biotrophic (oomycete *H. arabidopsidis* NoCo2), hemibiotrophic (bacteria *Pst* DC3000) and necrotrophic (fungus *Botrytis cinerea*) pathogens. The results clearly showed that resistance to these pathogens was dependent on a high SA content. Resistance to *H. arabidopsidis* NoCo2 and *Pst* DC3000 was perhaps not surprising as resistance to such pathogens is generally associated with SA signalling (Glazebrook, 2005). On the other hand, the role of SA in regulating resistance to necrotrophs is rather uncommon. Indeed, plant defence against necrotrophs is commonly associated with jasmonic acid signalling (Ferrari *et al.,* 2003; Glazebrook, 2005). However, Ferrari *et al.* (2003) showed that resistance to *B. cinerea* could be dependent on high SA levels, in accordance with our

observations. A similar finding was reported for defence response to the necrotroph *Sclerotinia sclerotiorum* (Novakova *et al.,* 2014). Moreover, we tested *A. thaliana* ETI by using a bacterial strain highly expressing the AvrRpt2 effector (*Pst* DC3000 AvrRpt2). An ETI response can induce the expression of genes commonly associated with SA, such as *PR-1*, in an SA-independent manner in *A. thaliana* (Tsuda *et al.,* 2013). Yet, we found that the higher resistance of *pi4kβ1β2* plants to *Pst* DC3000 AvrRpt2 was SA-dependent. In conclusion, the higher resistance of the *pi4kβ1β2* mutant to all the host pathogens assayed was strongly SA-dependent.

Non-host resistance, efficient against non-adapted pathogens, does not rely fully on the SA pathway. Here we show that *pi4kβ1β2* exhibited an SA-independent defective resistance towards penetration of the non-host pathogen *Bgh*.

Callose is a linear polysaccharide (1,3-*β*-glucan) occurring in plant cells where it is important for many plant physiological processes such as cytokinesis (Chen and Kim, 2009). Callose accumulation is triggered in response to pathogens and is used as a common test of pathogen-triggered immunity upon treatment with typical pathogen-associated molecular patterns such as flg22, the epitope of flagellin (Luna *et al.,* 2011). In mock inoculated *pi4k β1β2*, callose deposition was greater than in WT leaves, thus confirming the findings of Antignani *et al.* (2015). Interestingly, this was also true for the *sid2pi4kβ1β2* triple mutant when compared to *sid2* plants, thus indicating an SA-independent phenomenon. Following inoculation with flg22, an increase in callose deposition was observed in all genotypes tested, but this was still higher in *pi4kβ1β2* compared to WT leaves, and callose deposition was higher in *sid2pi4kβ1β2* with respect to *sid2* plants. Therefore, it seems that the *pi4kβ1β2* double mutation *per se* enabled higher callose deposition under biotic stress conditions.

The biosynthesis of callose occurs outside of the cell (Ellinger and Voigt, 2014). Accumulation can be regulated at different levels: transcriptional, translational, or during enzyme transport to the plasma membrane and out of the cell via vesicular trafficking. Phosphorylation and direct translocation of callose synthase is crucial in the regulation of biosynthesis, whereas transcriptional control might have only a minor role (Ellinger and Voigt, 2014). Our data on the transcription levels of *CALS1* and *CALS12* indicate that in *pi4kβ1β2* a transcriptional effect is not involved in the observed over-accumulation of callose. So how is it possible to explain the action on callose of the *pi4kβ1β2* double mutation *per se*? A number of reports indicate that PI4Ks can impact trafficking. In *A. thaliana*, PI4Kβ1 was shown to be recruited by the GTP-bound Rab4b GTPAse. Both RabA4b and PI4K*β1* localize to budding secretory vesicles in the trans-Golgi network (TGN) and to secretory vesicles *en route* to the cell surface. A *pi4kβ1β2* double mutant produces secretory vesicles of highly variable sizes (Preuss *et al.,* 2006; Kang *et al.,* 2011; Antignani *et al.,* 2015). The product of PI4K activity, PI4P massively accumulates at the plasma membrane and at early endosomes/TGN and Golgi (Platre and Jaillais, 2016; Noack and Jaillais, 2017). Therefore, PI4K*β1/β2* are important in vesicle trafficking. Interestingly, inhibiting PI4K with phenylarsine oxide (PAO) suppressed the salt-induced endocytosis of plasma membrane intrinsic protein 2;1 (Ueda *et al.,* 2016). Similarly, inhibiting PI4K led to the internalization of CELLULOSE SYNTHASE3 from the plasma
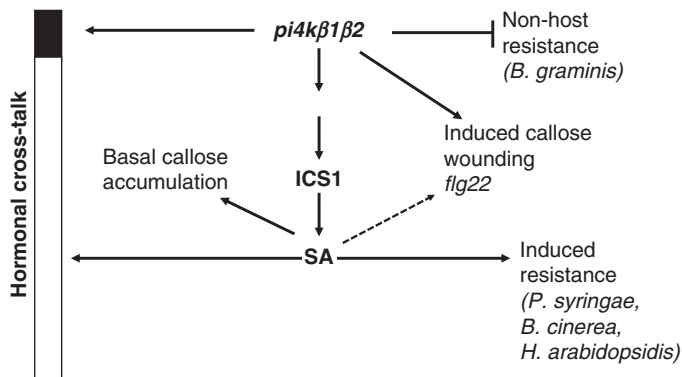
Fɪɢ. 6. Schematic representation of the effects of the *pi4kβ1β2* double mutation on Arabidopsis plants.

membrane (Fujimoto *et al.*, 2015). Can the impact of PI4K betas on trafficking explain the increased callose accumulation? Callose biosynthesis and accumulation have been shown to be affected by vesicle trafficking (Ellinger and Voigt, 2014). PI4Ks have been shown to play an important role in cytokinesis (Lin *et al.*, 2019), especially in the correct organization of the vesicles at the cell division pla *β1β2*ne and further formation of a cell plate. During phragmoplast formation, PI4Kβ1 probably interacts with MPK4, a member of the MAP65 protein family that regulates microtubule organization (Lin *et al.,*, 2019). Callose is also essential for cytokinesis (Thiele *et al.*, 2009). We can therefore only speculate whether the effects of PI4Ks on callose, cytokinesis and trafficking are interconnected. Interestingly, the role of SA in these processes has not been tested. Because PI4K*β1/β2* can impact the secretory pathway, they could also impact the translocation of callose synthases. Furthermore, PMR4 (CALS12) binds to small RabA4c GTPase at the TGN and PI4Kβ1 binds to RabA4b GTPase, the most similar small GTPase to RabA4c, at the TGN (Böhlenius *et al.*, 2010). Note that the impact of PI4K betas on trafficking could also explain our non-host resistance data. The *syp121* mutant altered in a SNARE protein involved in trafficking has been reported to accumulate SA and also display defective non-host resistance (Collins *et al.,*, 2003).

In conclusion (Fig. 6), the *pi4kβ1β2* double mutant constitutively accumulated a high SA level via ICS1/SID2 and this had considerable impact on other hormone levels and was associated with an increased resistance to several plant pathogens (*P. syringae*, *H. arabidopsidis*, *Botrytis cinerea*). The *pi4kβ1β2* double mutation also affected pathogen-related processes in a high SA-independent manner as seen by differences in callose accumulation in response to *flg22*, to *Bgh* infection, to wounding, and the higher penetration success of *Bgh*. The identification of such processes directly affected by the mutation on PI4Ks will now allow us to better investigate the role of these enzymes, in relation to signalling or trafficking events.

## SUPPLEMENTARY DATA

Supplementary data are available online at https://academic.oup.com/aob and consist of the following. Table S1: Phytohormone levels in 4-week-old plants. Fig. S1: Levels of hormones controlled by SA in 4-week-old mutant and WT plants. Fig. S2; Levels of hormones not controlled by SA in 4-week-old mutant and WT plants. Fig. S3: Resistance to *P. syringae* pv. *tomato* DC3000 AvrRpt2. Fig. S4: Callose deposition in response to wounding. Fig. S5: Relative transcription of some *CalS* genes in untreated rosette leaves or 24 h after infiltration with 0.1 μᴍ flg22.

## LITERATURE CITED

**Antignani V, Klocko AL, Bak G, Chandrasekaran SD, Dunivin T, Nielsen E. 2015.** Recruitment of PLANT U-BOX13 and the PI4Kbeta1/beta2 phosphatidylinositol-4 kinases by the small GTPase RabA4B plays important roles during salicylic acid-mediated plant defense signaling in Arabidopsis. *Plant Cell* **27**: 243–261.

**Assaad FF, Qiu JL, Youngs H, *et al.* 2004.** The PEN1 syntaxin defines a novel cellular compartment upon fungal attack and is required for the timely assembly of papillae. *Molecular Biology of the Cell* **15**: 5118–5129.

**Balla T. 2007.** Imaging and manipulating phosphoinositides in living cells. *Journal of Physiology* **582**: 927–937.

**Böhlenius H, Mørch SM, Godfrey D, Nielsen ME, Thordal-Christensen H. 2010.** The multivesicular body-localized GTPase ARFA1b/1c is important for callose deposition and ROR2 syntaxin-dependent preinvasive basal defense in barley. *The Plant Cell* **22**: 3831.

**Cao H, Glazebrook J, Clarke JD, Volko S, Dong X. 1997.** The Arabidopsis NPR1 gene that controls systemic acquired resistance encodes a novel protein containing ankyrin repeats. *Cell* **88**: 57–63.

**Collins NC, Thordal-Christensen H, Lipka V, *et al.* 2003.** SNARE-protein-mediated disease resistance at the plant cell wall. *Nature* **425**: 973–977.

**Cui H, Gobbato E, Kracher B, Qiu J, Bautor J, Parker JE. 2017.** A core function of EDS1 with PAD4 is to protect the salicylic acid defense sector in Arabidopsis immunity. *New Phytologist* **213**: 1802–1817.

**Czechowski T, Stitt M, Altmann T, Udvardi MK, Scheible WR. 2005.** Genome-wide identification and testing of superior reference genes for transcript normalization in Arabidopsis. *Plant Physiology* **139**: 5–17.

**Delage E, Ruelland E, Guillas I, Zachowski A, Puyaubert J. 2012.** Arabidopsis type-III phosphatidylinositol 4-kinases beta1 and beta2 are upstream of the phospholipase C pathway triggered by cold exposure. *Plant and Cell Physiology* **53**: 565–576.

**Delaney TP, Uknes S, Vernooij B, *et al.* 1994.** A central role of salicylic Acid in plant disease resistance. *Science* **266**: 1247–1250.

**Dempsey DMA, Vlot AC, Wildermuth MC, Klessig DF. 2011.** Salicylic Acid biosynthesis and metabolism. *Arabidopsis Book* **9**: e0156–e.

**Dobrev PI, Hoyerova K, Petrasek J. 2017.** Analytical determination of auxins and cytokinins. *Methods in Molecular Biology* **1569**: 31–39.

**Dobrev PI, Kaminek M. 2002.** Fast and efficient separation of cytokinins from auxin and abscisic acid and their purification using mixed-mode solid-phase extraction. *Journal of Chromatography A* **950**: 21–29.

**Dobrev PI, Vankova R. 2012.** Quantification of abscisic acid, cytokinin, and auxin content in salt-stressed plant tissues. *Methods in Molecular Biology* **913**: 251–261.

**Dong X, Hong Z, Chatterjee J, Kim S, Verma DP. 2008.** Expression of callose synthase genes and its connection with Npr1 signaling pathway during pathogen infection. *Planta* **229**: 87–98.

**Ellinger D, Glockner A, Koch J, *et al.* 2014.** Interaction of the Arabidopsis GTPase RabA4c with its effector PMR4 results in complete penetration resistance to powdery mildew. *Plant Cell* **26**: 3185–3200.

**Ellinger D, Voigt CA. 2014.** Callose biosynthesis in Arabidopsis with a focus on pathogen response: what we have learned within the last decade. *Annals of Botany* **114**: 1349–1358.

**Ferrari S, Plotnikova JM, De Lorenzo G, Ausubel FM. 2003.** Arabidopsis local resistance to Botrytis cinerea involves salicylic acid and camalexin and requires EDS4 and PAD2, but not SID2, EDS5 or PAD4. *Plant Journal* **35**: 193–205.

**Fujimoto M, Suda Y, Vernhettes S, Nakano A, Ueda T. 2015.** Phosphatidylinositol 3-kinase and 4-kinase have distinct roles in intracellular trafficking of cellulose synthase complexes in Arabidopsis thaliana. *Plant and Cell Physiology* **56**: 287–298.

**Glazebrook J. 2005.** Contrasting mechanisms of defense against biotrophic and necrotrophic pathogens. *Annual Review of Phytopathology* **43**: 205–227.

**Gross J, Cho WK, Lezhneva L, *et al.* 2006.** A plant locus essential for phylloquinone (vitamin K1) biosynthesis originated from a fusion of four eubacterial genes. *Journal of Biological Chemistry* **281**: 17189–17196.

**Chen XY, Kim JY. 2009.** Callose synthesis in higher plants. *Plant Signaling and Behaviour* **4**: 489–492.

**Jacobs AK, Lipka V, Burton RA, *et al.* 2003.** An Arabidopsis callose synthase, GSL5, is required for wound and papillary callose formation. *Plant Physiology* **15**: 2503–2313.

**Janda M, Sasek V, Ruelland E. 2014.** The Arabidopsis pi4kIIIbeta1beta2 double mutant is salicylic acid-overaccumulating: a new example of salicylic acid influence on plant stature. *Plant Signaling and Behaviour* **9**: e977210.

**Janda M, Ruelland E. 2015.** Magical mystery tour: salicylic acid signalling. *Environmental and Experimental Botany* **114**: 117–128.

**Kalachova T, Puga-Freitas R, Kravets V, *et al.* 2016.** The inhibition of basal phosphoinositide-dependent phospholipase C activity in Arabidopsis suspension cells by abscisic or salicylic acid acts as a signalling hub accounting for an important overlap in transcriptome remodelling induced by these hormones. *Environmental and Experimental Botany* **123**: 37–49.

**Kang BH, Nielsen E, Preuss ML, Mastronarde D, Staehelin LA. 2011.** Electron tomography of RabA4b- and PI-4Kbeta1-labeled trans Golgi network compartments in Arabidopsis. *Traffic* **12**: 313–329.

**Katagiri F, Thilmony R, He SY. 2002.** The Arabidopsis thaliana-pseudomonas syringae interaction. *Arabidopsis Book* **1**: e0039.

**Kohler A, Schwindling S, Conrath U. 2002.** Benzothiadiazole-induced priming for potentiated responses to pathogen infection, wounding, and infiltration of water into leaves requires the NPR1/NIM1 gene in Arabidopsis. *Plant Physiology* **128**: 1046–1056.

**Krinke O, Ruelland E, Valentová O, *et al.* 2007.** Phosphatidylinositol 4-Kinase activation is an early response to salicylic acid in Arabidopsis suspension cells. *Plant Physiology* **144**: 1347–1359.

**Krinke O, Flemr M, Vergnolle C, *et al.* 2009.** Phospholipase D activation is an early component of the salicylic acid signaling pathway in Arabidopsis cell suspensions. *Plant Physiology* **150**: 424–436.

**Lee H-A, Lee H-Y, Seo E, *et al.* 2017.** Current understandings of plant Nonhost Resistance. *Molecular Plant–Microbe Interactions* **30**: 5–15.

**Lin F, Krishnamoorthy P, Schubert V, Hause G, Heilmann M, Heilmann I. 2019.** A dual role for cell plate-associated PI4Kβ in endocytosis and phragmoplast dynamics during plant somatic cytokinesis. *The EMBO Journal* **38**: e100303.

**Luna E, Pastor V, Robert J, Flors V, Mauch-Mani B, Ton J. 2011.** Callose deposition: a multifaceted plant defense response. *Molecular Plant–Microbe Interactions* **24**: 183–193.

**Marshall OJ. 2004.** PerlPrimer: cross-platform, graphical primer design for standard, bisulphite and real-time PCR. *Bioinformatics* **20**: 2471–2472.

**Mega R, Meguro-Maoka A, Endo A, *et al.* 2015.** Sustained low abscisic acid levels increase seedling vigor under cold stress in rice (*Oryza sativa* L.). *Scientific Reports* **5**: 13819.

**Mosher S, Moeder W, Nishimura N, *et al.* 2010.** The lesion-mimic mutant cpr22 shows alterations in abscisic acid signaling and abscisic acid insensitivity in a salicylic acid-dependent manner. *Plant Physiology* **152**: 1901–1913.

**Nakanishi S, Catt KJ, Balla T. 1995.** A wortmannin-sensitive phosphatidylinositol 4-kinase that regulates hormone-sensitive pools of inositolphospholipids. *Proceedings of the National Academy of Sciences of the USA* **92**: 5317–5321.

**Noack LC, Jaillais Y. 2017.** Precision targeting by phosphoinositides: how PIs direct endomembrane trafficking in plants. *Current Opinion in Plant Biology* **40**: 22–33.

**Normanly J. 2010.** Approaching cellular and molecular resolution of auxin biosynthesis and metabolism. *Cold Spring Harbor Perspectives in Biology* **2**: a001594.

**Novakova M, Sasek V, Dobrev PI, Valentova O, Burketova L. 2014.** Plant hormones in defense response of *Brassica napus* to *Sclerotinia sclerotiorum* - reassessing the role of salicylic acid in the interaction with a necrotroph. *Plant Physiology and Biochemistry* **80**: 308–317.

**Pappan K, Austin-Brown S, Chapman KD, Wang X. 1998.** Substrate selectivities and lipid modulation of plant phospholipase D alpha, -beta, and -gamma. *Archives of Biochemistry and Biophysics* **353**: 131–140.

**Platre MP, Jaillais Y. 2016.** Guidelines for the use of protein domains in acidic phospholipid imaging. *Methods in Molecular Biology* **1376**: 175–194.

**Preuss ML, Schmitz AJ, Thole JM, Bonner HK, Otegui MS, Nielsen E. 2006.** A role for the RabA4b effector protein PI-4Kbeta1 in polarized expansion of root hair cells in *Arabidopsis thaliana*. *Journal of Cell Biology* **172**: 991–998.

**R Core Team. 2014.** *R: A language and environment for statistical computing*. Vienna: R Foundation for Statistical Computing.

**Sasek V, Janda M, Delage E, *et al.* 2014.** Constitutive salicylic acid accumulation in pi4kIIIbeta1beta2 Arabidopsis plants stunts rosette but not root growth. *New Phytologist* **203**: 805–816.

**Seyfferth C, Tsuda K. 2014.** Salicylic acid signal transduction: the initiation of biosynthesis, perception and transcriptional reprogramming. *Frontiers in Plant Science* **5**: 697.

**Takemoto D, Jones DA, Hardham AR. 2006.** Re-organization of the cytoskeleton and endoplasmic reticulum in the Arabidopsis pen1-1 mutant inoculated with the non-adapted powdery mildew pathogen, *Blumeria graminis f. sp. hordei*. *Molecular Plant Pathology* **7**: 553–563.

**Thiele K, Wanner G, Kindzierski V, *et al.* 2009.** The timely deposition of callose is essential for cytokinesis in Arabidopsis. *The Plant Journal* **58**: 13–26.

**Tsuda K, Mine A, Bethke G, *et al.* 2013.** Dual regulation of gene expression mediated by extended MAPK activation and salicylic acid contributes to robust innate immunity in Arabidopsis thaliana. *PLoS Genetics* **9**: e1004015.

**Ueda M, Tsutsumi N, Fujimoto M. 2016.** Salt stress induces internalization of plasma membrane aquaporin into the vacuole in *Arabidopsis thaliana*. *Biochemical and Biophysical Research Communications* **474**: 742–746.

**Vlot AC, Dempsey DA, Klessig DF. 2009.** Salicylic acid, a multifaceted hormone to combat disease. *Annual Review of Phytopathology* **47**: 177–206.

**Vogel J, Somerville S. 2000.** Isolation and characterization of powdery mildew-resistant Arabidopsis mutants. *Proceedings of the National Acadademy of Sciences USA* **97**: 1897–1902.

**Voigt CA. 2014.** Callose-mediated resistance to pathogenic intruders in plant defense-related papillae. *Frontiers in Plant Science* **5**: 168.

**Wagner S, Stuttmann J, Rietz S, *et al.* 2013.** Structural basis for signaling by exclusive EDS1 heteromeric complexes with SAG101 or PAD4 in plant innate immunity. *Cell Host & Microbe* **14**: 619–630.

**Wildermuth MC, Dewdney J, Wu G, Ausubel FM. 2001.** Isochorismate synthase is required to synthesize salicylic acid for plant defence. *Nature* **414**: 562–565.

**Yi SY, Shirasu K, Moon JS, Lee SG, Kwon SY. 2014.** The activated SA and JA signaling pathways have an influence on flg22-triggered oxidative burst and callose deposition. *PLoS One* **9**: e88951.